Lowfrequency Raman scattering and structure of amorphous polymers: Stretching effect

T. Achibat, A. Boukenter, E. Duval, G. Lorentz, and S. Etienne

Citation: The Journal of Chemical Physics **95**, 2949 (1991); doi: 10.1063/1.460896
View online: http://dx.doi.org/10.1063/1.460896
View Table of Contents: http://scitation.aip.org/content/aip/journal/jcp/95/4?ver=pdfcov
Published by the AIP Publishing

Articles you may be interested in

Low-frequency Raman scattering from silicon nanostructures
J. Appl. Phys. **110**, 064317 (2011); 10.1063/1.3633235

LowFrequency Raman Scattering by Acoustic Vibrations of Anisotropic Nanoparticles
AIP Conf. Proc. **1267**, 259 (2010); 10.1063/1.3482500

Dynamical structure of water in dioxane aqueous solution by lowfrequency Raman scattering
J. Chem. Phys. **104**, 7377 (1996); 10.1063/1.471479

Dynamical structure of water in aqueous electrolyte solutions by lowfrequency Raman scattering
J. Chem. Phys. **101**, 3453 (1994); 10.1063/1.467530

Dynamical structure of water: Lowfrequency Raman scattering from a disordered network and aggregates
J. Chem. Phys. **92**, 2150 (1990); 10.1063/1.458006

This article is copyrighted as indicated in the article. Reuse of AIP content is subject to the terms at: http://scitation.aip.org/termsconditions. Downloaded to IP: 137.189.170.231 On: Mon, 22 Dec 2014 19:13:10

Low-frequency Raman scattering and structure of amorphous polymers: Stretching effect

T. Achibat, A. Boukenter, and E. Duval
Laboratoire de Physicochimie des Matériaux Luminescents, URA CNRS 442, Université Lyon I, Campus La Doua, 69622 Villeurbanne, France

G. Lorentz
CRC, Rhône-Poulenc, 85 av des Frères Perret, BP 62 69192 Saint Fons Cedex, France

S. Etienne
GEMPPM, URA-CNRS 341, INSA, 69621 Villeurbanne, France

(Received 22 January 1991; accepted 7 May 1991)

Low-frequency Raman scattering of amorphous polymers [polyethyleneterephthalate (PET) and polymethylmethacrylate] is investigated. The low-frequency Raman band called "Boson peak" is interpreted in terms of a noncontinuous structure, similar to that of inorganic glasses, i.e., solid amorphous polymers are composed of 50 Å blobs. These are related blobs to transient entanglements in the polymer melt. Modifications induced by stretching are described for a PET film. The nature of the blob structure is discussed.

I. INTRODUCTION

Low-energy excitations in amorphous solid polymers present universal glass characteristics particularly a specific heat larger than the predicted Debye variation,[1] and a plateau[2,3] of their thermal conductivity. These two thermal anomalies have been correlated to an "excess" of the density of vibrational states (DVS) as, for example, observed by inelastic neutron scattering,[4,5] and low-frequency Raman scattering ("Boson peak").[6,7]

In a recent paper, Duval *et al.*[8] suggested that the observed DVS could be explained by a noncontinuous structure of glasses, i.e., by the existence of blobs. The presence of such blobs in inorganic glasses, which can be deduced from inelastic neutron scattering and low-frequency inelastic (Raman) light scattering (LOFIS) experiments, has been explained by a stronger bonding between atoms in blobs than between atoms in different nearest-neighbor blobs.[8] Because the lattice of blobs is not necessarily in phase with density fluctuations, it is difficult to observe by classical techniques such as electronic microscopy and small angle (neutron or x ray) scattering. The same features have been observed for solid amorphous polymers and for organic glasses: a maximum of inelastic neutron scattering at low energy[9,10] and a "Boson peak" in LOFIS,[11-13] which lead to the proposal that structural units, similar to the blobs in inorganic glasses, exist in solid amorphous polymers.

The noncontinuous structure of polymer glass, as revealed by its vibrational properties, has to be related to the well-known entangled structure which has successfully explained the mechanical and transport properties of polymer melts.[14,15] We will suggest that a memory of the transient entanglements of the melt persists in the glass after freezing. The size of the blobs that we observe in LOFIS would, therefore, be equal to the distance between entanglements.

In this paper we present LOFIS experimental results obtained from polyethyleneterephthalate (PET) films. They were compared to results obtained from other polymer glasses like polymethylmethacrylate (PMMA) or polystyrene (PS). The effect of stretchings, which induce a crystallization, is particularly discussed.

II. EXPERIMENTAL

The sample of PET was provided by Rhône–Poulenc Films. Standard filler-free PET was extruded and quenched on a chill roll at a temperature of 20 °C. The obtained film was amorphous and isotropic, as indicated by the refractive indices $n_1 = n_2 = n_3 = 1.575$ (measured with an Abbe refractometer).

The average molecular weight was 39 000, as determined by viscosimetry in orthochloro-phenol at 25 °C. The *Tg* of the polymer was measured with a Dupont 1090 analyzer and found to be 80 °C at 20 °C/min. The oriented samples were obtained on a pilot installation with a balanced process.

Three PET films were compared: (1) an isotropic and amorphous film with a thickness of 170 μm and a crystallinity <0.005; (2) a uniaxial-planar drawn film with a thickness of 90 μm, a draw ratio $\lambda = 2.9$, an axial birefringence $\Delta n = 0.045$, and a crystallinity $X \cong 0.035$; (3) a uniaxial-planar drawn film with a thickness of 50 μm, $\lambda = 3.4$, $\Delta n = 0.0875$, and $X = 0.14$. For films (2) and (3) the drawing was carried out at a temperature above *Tg*. The studied PMMA was atactic with an average molecular weight of 63 000.

The laser beam was guided in the PET film. To avoid the fluorescence which appeared with the blue and green lines of the Ar laser, a red laser was preferred. Consequently, the 6328 Å line of a He–Ne laser and the 6471 Å of a Kr laser were chosen to excite the samples. The beam powers were, respectively, 25 and 100 mW. The Raman scattering was observed along a direction perpendicular to the laser beam and the film surface. A U1000 double monochromator (Jobin–Yvon) and a photon counting system were used to analyze the scattered light. The light rejection of the monochromator was 10^{-14} at 20 cm^{-1} from the Rayleigh line, the dispersion was 9.2 cm^{-1}/mm and the resolution was <0.15 cm^{-1}. The width of the slits was no larger than 250 μm. The

This article is copyrighted as indicated in the article. Reuse of AIP content is subject to the terms at: http://scitation.aip.org/termsconditions. Downloaded to IP: 137.189.170.231 On: Mon, 22 Dec 2014 19:13:10

 0021-9606/91/162949-06$03.00 © 1991 American Institute of Physics

Raman low-frequency spectra observed with a new Dilor quintuple monochromator, with a 4 m focal length, were identical. The Rayleigh line wings, therefore, do not modify the observed low-frequency spectra.

III. RESULTS

Figure 1 shows the Raman–Stokes intensity $I(\omega)$ of amorphous PET from 3 to 180 cm^{-1}, and the reduced intensity $I(\omega)/[n(\omega)+1]$, where $[n(\omega)+1]$ is the Bose factor. In the reduced spectrum two features are observed: a maximum at 57.5 cm^{-1} and a shoulder at 20 cm^{-1}. This shoulder is related to the maximum at 10 cm^{-1} in the direct spectrum $I(\omega)$. LOFIS spectra and $I(\omega)/[n(\omega)+1]$ of PMMA glass can be seen in Fig. 2. The same features are observed: a low-energy peak for $I(\omega)$ at 16 cm^{-1}, a broadband with a maximum at 80 cm^{-1}, and a shoulder at 20 cm^{-1} in $I(\omega)/[n(\omega)+1]$.

In a preceding paper[16] it was shown that the broadband which appears in $I(\omega)/[n(\omega)+1]$ corresponds to the scattering from acoustical modes localized by the disorder. The broadband which has a maximum at 57.5 cm^{-1} in amorphous PET transforms into two narrow bands with maxima at 76 and 129 cm^{-1}, respectively, after partial crystallization of the film upon stretching. Both bands were clearly observed for precise polarizations of the laser and scattering beams, in particular when the polarization of the laser beam was perpendicular to the film and the polarization of the scattered beam was perpendicular to the drawing direction. They were attributed to crystalline acoustic modes: the highest energy band to longitudinal modes, and the lowest one to transverse modes. Comparison with amorphous films shows that disorder induces a broadening and a low-energy shift of the acoustic bands: the longitudinal modes are not separated from the transverse modes in the scattering from amorphous PET films.

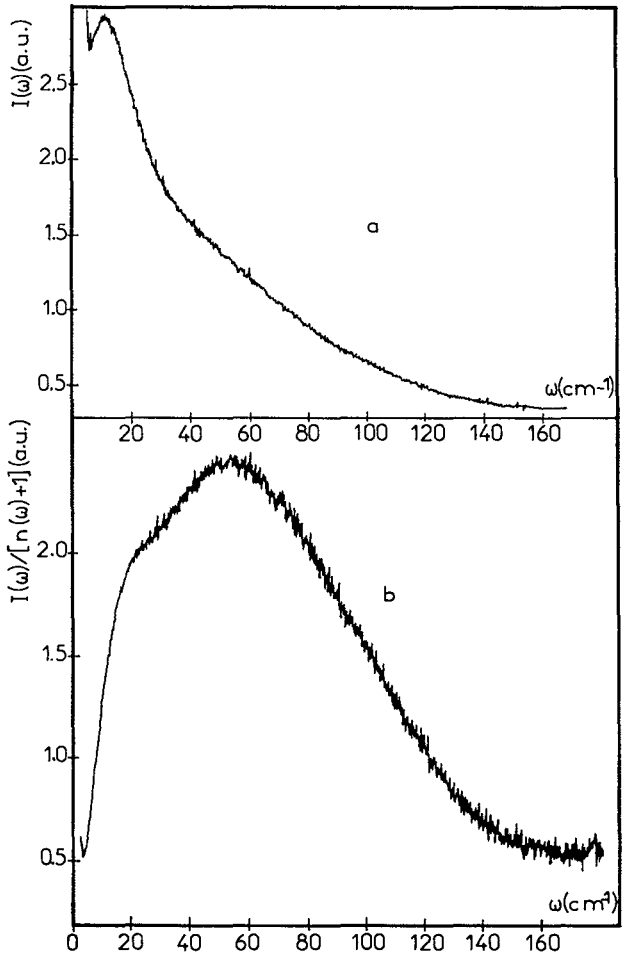

FIG. 1. Low-frequency Raman scattering from amorphous PET: (a) $I(\omega)$ and (b) $I(\omega)/[n(\omega)+1]$.

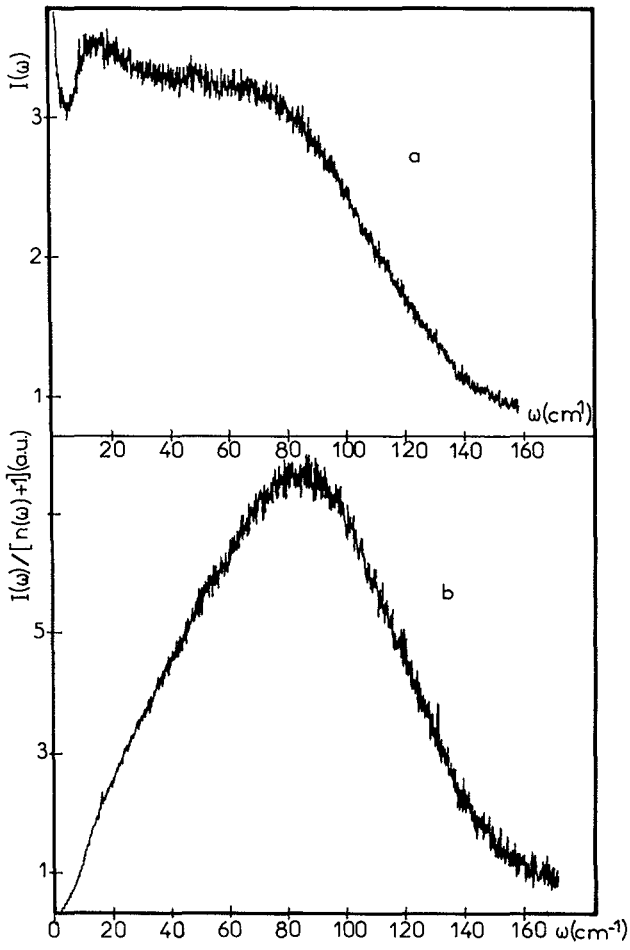

FIG. 2. Low-frequency Raman scattering from PMMA: (a) $I(\omega)$ and (b) $I(\omega)/[n(\omega)+1]$.

The lowest-energy maximum of $I(\omega)$ at ~ 10 cm^{-1} for the PET and 16 cm^{-1} for the PMMA (Figs. 1 and 2) corresponds to the so-called Boson peak in inorganic glasses. In $I(\omega)/[n(\omega)+1]$ this maximum is reduced into a shoulder on the low-energy wing of acoustic band. Such an attribution should be done with caution because it is possible to observe a low-energy maximum in $I(\omega)$ without any corresponding definite feature in the reduced intensity $I(\omega)/[n(\omega)+1]$. This is the case for amorphous polyvinychloride (PVC).[13,17]

To make a precise interpretation of the Boson peak, or of the low-energy shoulder in the reduced intensity, we have

This article is copyrighted as indicated in the article. Reuse of AIP content is subject to the terms at: http://scitation.aip.org/termsconditions. Downloaded to IP: 137.189.170.231 On: Mon, 22 Dec 2014 19:13:10

studied the effect of stretching which induces a partial crystallization of the PET film. In Fig. 3 the LOFIS $I(\omega)$ of amorphous and stretched films are compared. LOFIS from the stretched film was observed for different polarization configurations. Following the standard notation, M (machine) specifies the stretching direction in the film, T (transverse) the direction perpendicular to M, parallel to the film, and N (normal) the direction perpendicular to the film. The configuration (TMMN) means that the laser excitation beam is along the T direction, polarizations of laser and scattered light are along the M direction, and propagation of the observed scattered light is along the N direction.

Obviously the LOFIS of the amorphous nonstretched film (1) was independent of the polarization configuration. On the contrary the anisotropy induced by the drawing in the films (2) and (3) is reflected in the LOFIS. In Fig. 3, a shift towards the Rayleigh line is observed for the Boson peak in (TNMN) configuration relative to the one in (TMMN). It is larger for film (3): it increases with the anisotropy (Δn). On the other hand the Boson peak of stretched films does not appear shifted in (TMMN), relative to the amorphous film.

It is probable that the observed shifts are due to the orientation and not to the crystallization for the following reasons: (1) the crystallinity of film (2) is low ($X = 0.035$); (2) it has been observed[16] that the LOFIS from acoustic bands of PET crystallites in stretched films appears in the (TNTN) configuration and not in (TNMN). Therefore, we conclude that the observed shifts in the (TNMN) configuration are due to the orientation of the amorphous structure.

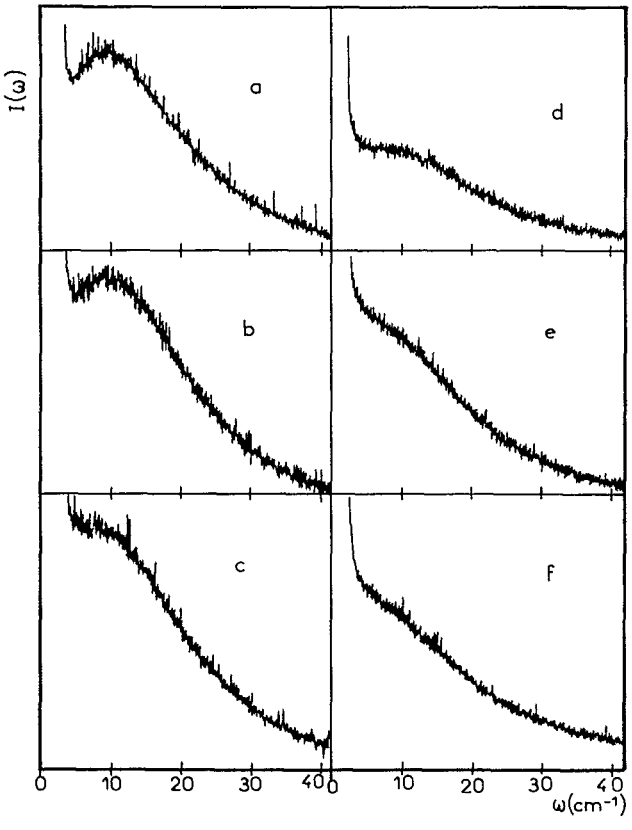

FIG. 3. Low-frequency Raman scattering from PET films: (a) amorphous film; (b) drawn film, $\lambda = 2.9$ (TMMN) polarization configuration; (c) $\lambda = 2.9$ (TNMN); (d) $\lambda = 3.4$ (TMMN); (e) $\lambda = 3.4$ (TNMN); (f) $\lambda = 3.4$ (TNTN).

IV. MODEL AND INTERPRETATION

The model has been described in a preceding paper[8] concerning the interpretation of the LOFIS and inelastic neutron scattering of inorganic glasses. It was assumed that a glass has a noncontinuous structure due to a stronger bonding between atoms in blobs than between atoms in different nearest-neighbor blobs. Such a structure has an effect on the effective DVS.

A. The model

We briefly recall the model. The size of a blob is $2a$. The size distribution of blobs is symbolized by the function $f(a)$. The lowest-energy vibration mode localized in a blob has a frequency ω_0 such that[18,8]

$$\omega_0 = S\frac{v}{2a}, \tag{1}$$

where v is the sound velocity in a blob and S is a shape factor. Therefore, the size distribution corresponds to a frequency distribution of the blob fundamental modes. We define a distribution $F(\omega_0)$, which is such that $F(\omega_0)d\omega_0$ is the ratio of the volume occupied in the glass by the blobs, fundamental mode frequencies of which are included between ω_0 and $\omega_0 + d\omega_0$, with respect to the glass sample volume.

Vibrations of long wavelengths, i.e., much longer than the mean value of $2a$, consist of the oscillations of blobs around their equilibrium position. Their delocalization or localization depends on the disorder in the blobs aggregates and the corresponding correlation length. When the vibration wavelength becomes double of the size $2a$ the vibrations localize in the blobs. If $g(\omega)$ is the real DVS inside the blobs, the effective DVS $g_{\text{eff}}(\omega)$ of vibrations localized in blobs which is observed is

$$g_{\text{eff}}(\omega) = g(\omega)\int_0^{\omega} F(\omega_0)d\omega_0. \tag{2}$$

If ω_1 is the upper limit for the frequency ω_0, which corresponds to the smaller size of blobs, for $\omega > \omega_1$, $g_{\text{eff}}(\omega)$ is simply proportional to $g(\omega)$,

$$g_{\text{eff}}(\omega) \propto g(\omega). \tag{3}$$

From the pioneering works[6,7] on Raman scattering from disordered materials, and expression (2), the reduced Raman intensity can be expressed as

$$\frac{I(\omega)}{n(\omega)+1} = \frac{C(\omega)}{\omega} g_{\text{eff}}(\omega). \tag{4}$$

For $\omega > \omega_1$, $\dfrac{I(\omega)}{n(\omega)+1}$ is proportional to $C(\omega)g(\omega)$.

B. Interpretation

In Fig. 4 are represented the log–log plot of $I(\omega)/[n(\omega)+1]$, amorphous PET (Fig. 1) and PMMA (Fig. 2). For PMMA, a perfect straight line is observed, from 20 cm^{-1} up to 65 cm^{-1}, with a slope $= 0.8$. The linear

This article is copyrighted as indicated in the article. Reuse of AIP content is subject to the terms at: http://scitation.aip.org/termsconditions. Downloaded to IP: 137.189.170.231 On: Mon, 22 Dec 2014 19:13:10

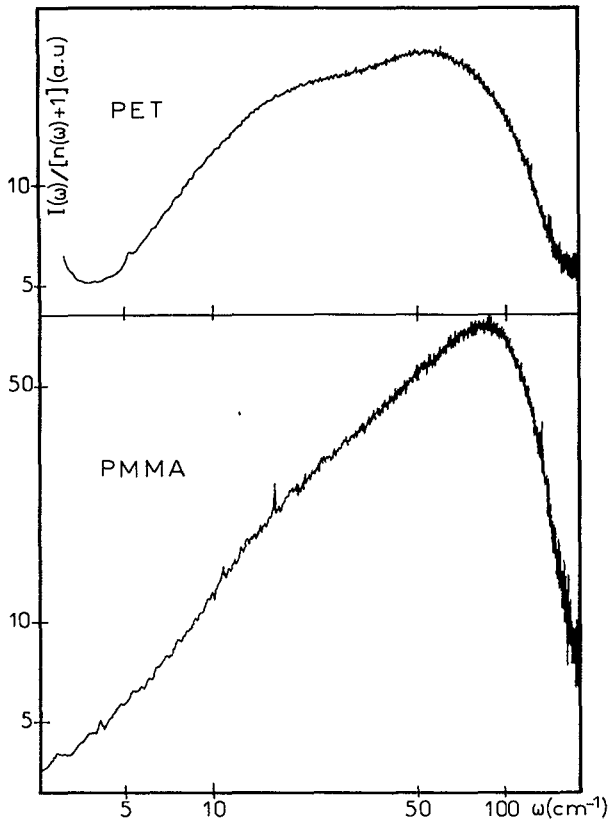

FIG. 4. Log–log plot of the reduced intensity $I(\omega)/[n(\omega)+1]$: (a) amorphous PET and (b) PMMA.

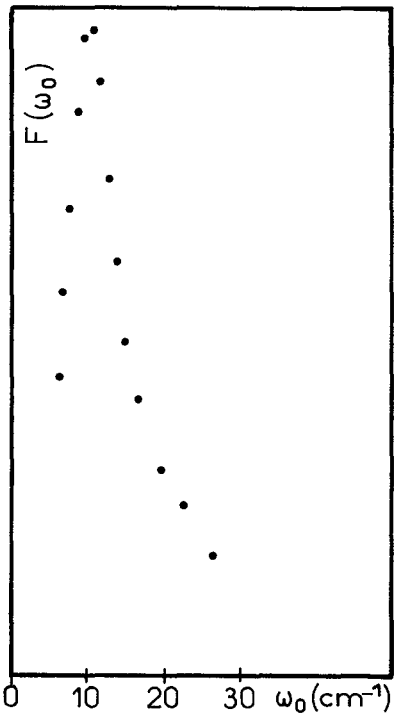

FIG. 5. $F(\omega_0)$ frequency distribution in PMMA.

part of the log–log plot, from 15 cm^{-1}, is narrow for PET. There is a slight increase of the slope between 35 and 50 cm^{-1}. This different behavior for PMMA and PET will be discussed later. If we assume a bell-shaped curve for $F(\omega_0)$, we find $F(\omega_0)\simeq 0$ from $\omega_0=\omega_1=20$ and 15 cm^{-1} for PMMA and PET, respectively. From the frequency ω_1, for the linear part, it can be written

$$C(\omega)g(\omega)\simeq\omega^x. \tag{5}$$

From Fig. 4, we obtain $x=1.8$ for PMMA and 1.3 for PET. From the expressions (2) and (4), dividing $I(\omega)/[n(\omega)+1]$ by ω^{x-1}, we obtain the integral of the distribution $F(\omega_0)$. It is assumed that x is a constant for the internal vibrations of the blobs.

Finally the distribution $F(\omega_0)$ is given by the derivative of $I(\omega)/[n(\omega)+1]\omega^{1-x}$. The distribution $F(\omega_0)$ for the PMMA sample is given in Fig. 5. The maximum of the distribution ω_m is 9.5 ± 1 cm^{-1}. The determination of ω_m for amorphous PET (Fig. 6) is less precise since the Boson peak is close to the Rayleigh line: one obtains $\omega_m=7.5\pm 2$ cm^{-1}. For the stretched films no measurable shift was observed in the (TMMN) configuration (Figs. 3 and 6). In the (TNMN) configuration, a shift towards the Rayleigh line is clearly observed (Fig. 3), but it was not possible to measure this shift exactly.

From Eq. (1) ω_m is correlated to the maximum $2a_m$ of the size distribution of the blobs. To deduce $2a_m$ from ω_m, the shape factor S has to be precised. $S\simeq 0.8$ for a spherical

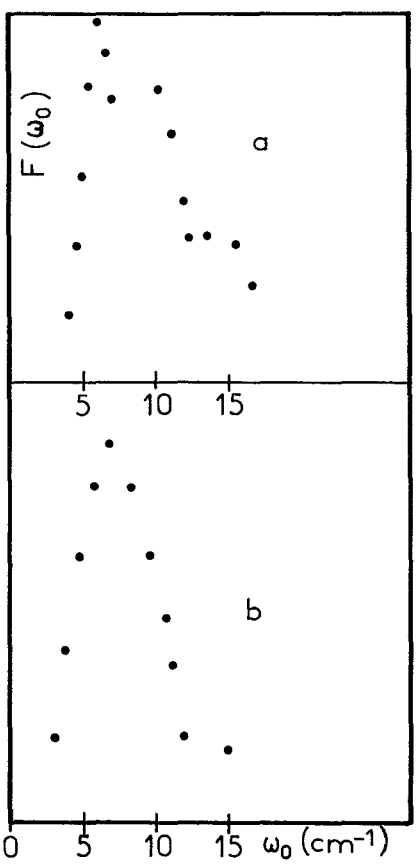

FIG. 6. $F(\omega_0)$ frequency distribution in PET films: (a) amorphous film and (b) drawn film, $\lambda=3.4$ (TMMN).

This article is copyrighted as indicated in the article. Reuse of AIP content is subject to the terms at: http://scitation.aip.org/termsconditions. Downloaded to IP: 137.189.170.231 On: Mon, 22 Dec 2014 19:13:10

shape and 0.5 for a linear object. We take here a mean value: $S = 0.65$. The measured sound velocity was $v = 1840$ m/s for PET and $V \simeq 2000$ m/s for PMMA. From Eq. (1) it is then found that $2a_m = 55 \pm 15$ Å for PET and $2a_m = 46 \pm 5$ Å for PMMA.

V. DISCUSSION

The maximum $2a_m$ of the size distribution of the blobs is not very different from the value of entanglement spacings in the corresponding polymer melts, as determined from the plateau modulus.[15,19,20] The latter is related to the mean number N_e of polymer bonds of length l between entanglements points. The entanglement spacing ξ is given by the following relation:[20]

$$\xi = N_e^{1/2} C_\infty^{1/2} l. \tag{6}$$

Using the plateau modulus value determined by Lebourvellec[21] for a PET, a ξ value of 31 Å is found from Eq. (6). For the PMMA, N_e was found to be ~ 80. Graessley and Edwards[19] calculated a $C_\infty = 8.7$, from which we find $\xi = 41$ Å. Considering the uncertainties about the values of the plateau moduli and ξ it is reasonable to assume that there exists a relationship between $2a_m$ and ξ. This means that the memory of the transient entanglements is preserved when the melt solidifies into a glass.

The anisotropy in uniaxial-planar drawn PET films is reflected in the shift of the Boson peak in the (TMMN) configuration with respect the one in (TNMN). In the (TNMN) configuration the maximum of $F(\omega_0)$, like the Boson peak, shifts towards the Rayleigh line as the drawing increases (Fig. 3). Within the framework of our model it means that the entanglement spacing increases along the drawing direction.

Other measurements of LOFIS were carried out on PS[22] and PVC.[17] LOFIS from PS was measured at low temperature (100 K) to avoid the broadening at the base of the Rayleigh line, due to relaxation modes,[9] which partially masks the phonon scattering at room temperature. From the experimental values $\omega_m = 7\ \text{cm}^{-1}$, $v = 1700$ m/s, and using expression (1), it was found that $2a_m = 53$ Å for PS. From the expression (6) and values of N_e, C_∞, and l, given in Ref. 20, ξ was found equal to 76 Å. The comparison between these values of ξ and $2a_m$, for PS, is another indication of the entanglement memory effect occurring at the melt-glass transition.

The LOFIS of PVC does not show the same characteristics as the other amorphous polymers,[13,17] since no maximum appears in $F(\omega_0)$. Two different explanations can tentatively be given for this experimental results: (1) the maximum of $F(\omega_0)$ is at very low energy and cannot be separated from the Rayleigh line; the size of the blobs would then be very large; (2) the entanglement memorization does not apply. The LOFIS of PVC was explained[17] by the existence of a close-packed three-dimensional continuous structure of the amorphous network[23] due to the ordered (or crystalline) structure at the scale of the vinyl chloride molecular unit. This hypothesis is supported by the fact that PVC is difficult to obtain purely amorphous.

Concerning the effect of crystallites, it was noticed that for a biaxially drawn PET film, with a crystallinity $X = 0.47$, the Boson peak was no more observed. The bonding with the crystallites therefore modifies the structure of the amorphous phase.

Viras and King[13] used, to interpret the Boson peak in LOFIS of amorphous polymers, a model in which the maximum of the Boson peak in $I(\omega)$ is directly related to a correlation length. This model is similar to that developed by Martin and Brenig[24] and was shown to be incorrect.[8] The sizes of blobs which could be deduced from their correlation lengths are about half our values for $2a_m$.

Reminiscent of the Boson peak, a maximum is observed in inelastic neutron scattering from amorphous polymer.[9] The correspondence between the Boson peak and the maximum in low-energy inelastic scattering was demonstrated for inorganic glasses.[8] We have not measured the inelastic neutron scattering from our samples. However, using the neutron data obtained for polybutadiene,[9] and applying our model,[8] we find $2a_m = 45 \pm 5$ Å. From Eq. (6) and Ref. 20, a ξ of 40 Å is obtained. This is one more example which shows the equivalence of $2a_m$ and ξ.

A last point that we have to discuss briefly in this paper concerns PMMA. A perfect linear variation of $I(\omega)/[n(\omega)+1]$ vs ω was observed for this polymer from 20 cm^{-1} up to 65 cm^{-1}, in a log–log plot (Fig. 4), with a slope $x = 0.8$, at room temperature. The same observation was reported by Malinovksy *et al.*[12] This perfect linear variation was observed at any temperature from -210 °C up to 140 °C, beyond the glass temperature transition. The slope x decreases with the temperature from 1 at -210 °C to 0.6 at 140 °C. A clear characteristic is indicative of the presence of fractions or localized (in a noncompact disordered material) vibrational modes. It was shown that[25,26]

$$x = \frac{2d}{D} + d - 2, \tag{7}$$

where D and d are the fractal and fracton dimensionalities, respectively. We have assumed in Eq. (7) that the superlocalization exponent $= 1$, which is presently the minimum hypothesis.[27]

Choosing $D = 2$ for percolation, it is found that $d = 1.5$ at -210 °C; with $D = 3$, $d = 1.8$. This value of d is in perfect agreement with the inelastic neutron measurements of Zwemlyanov *et al.*[28]

No such perfect linear variation was observed for PET and PS. This means that the structure of blobs or entanglements is different in the two types of polymers: fractal in PMMA, nonfractal and probably close packed at short distances in PET and PS. On the other hand, a similarly perfect linear variation was observed in amorphous DGEBA (diglcycidyl ether of bisphenol A) and epoxy resin.[29]

VI. CONCLUSION

Like inorganic glasses,[8] amorphous polymers exhibit a shoulder on the low-frequency wing of the Raman band, corresponding to the scattering from localized acoustic modes. It has been shown that this feature is related to the blob structure of the amorphous polymers. The size of the blobs is close to the entanglement spacings of the polymer

This article is copyrighted as indicated in the article. Reuse of AIP content is subject to the terms at: http://scitation.aip.org/termsconditions. Downloaded to IP: 137.189.170.231 On: Mon, 22 Dec 2014 19:13:10

melt. It is concluded that there exists a relationship between blobs in the amorphous solid and entanglements in the polymer melt.

In the uniaxial-planar drawn PET films, the LOFIS is anisotropic. It shows that the entanglement spacing is larger in the drawing direction and increases with the draw ratio.

The origin of the low-frequency Raman shoulder (Boson peak) is the same as the low-frequency band of inelastic neutron scattering.[9]

The frequency variation of the Raman scattering from acoustic modes reveals a fracton behavior of vibrations of the elastic network in blobs of PMMA.

ACKNOWLEDGMENTS

The authors acknowledge the Ministère de la Recherche et Technologie for financial support. They are grateful to E. Roche for fruitful discussions.

[1] R. O. Pohl, in *Amorphous Solids* (Springer, Berlin, 1981), Chap. 3.
[2] A. C. Anderson, in *Amorphous Solids* (Springer, Berlin, 1981), Chap 5.
[3] J. E. Graebner, B. Golding, and L. C. Allen, Phys. Rev. B **34**, 5696 (1986).
[4] V. Buchenau, M. Prager, N. Nucker, A. J. Dianoux, N. Ahmad, and W. A. Phillips, Phys. Rev. B **34**, 5665 (1986).
[5] V. K. Malinovsky, V. N. Novikov, P. P. Parshin, A. P. Sokolov, and M. G. Zemlyanov, Europhys. Lett. **11**, 43 (1990).
[6] R. Shuker and R. W. Gammon, Phys. Rev. Lett. **25**, 222 (1970).
[7] J. Jäckle, in *Amorphous Solids* (Springer, Berlin, 1981), Chap. 8.
[8] E. Duval, A. Boukenter, and T. Achibat, J. Phys. Condensed Matter **2**, 10 277 (1990).
[9] B. Frick and D. Richter, in *Dynamics of Disordered Materials*, Vol. 39 in Springer Proceedings in Physics (Springer, New York, 1989), p. 38.
[10] B. Frick, Prog. Colloid and Poly. Sci. **80**, 164 (1989).
[11] S. J. Spells and I. W. Shepherd, J. Chem. Phys. **66**, 1427 (1977).
[12] V. K. Malinovsky, V. N. Novikov, A. P. Sokoliv, and V. A. Bagryansky, Chem. Phys. Lett. **143**, 111 (1988).
[13] F. Viras and T. A. King, J. Non-Cryst. Solids **119**, 65 (1990).
[14] W. W. Graessley, Adv. Polym. Sci. **16**, 1 (1974).
[15] J. D. Ferry, in *Viscoelastic Properties of Polymers* (Wiley, New York, 1980).
[16] A. Boukenter, T. Achibat, E. Duval, G. Lorentz, and J. Beautemps, Polymer Comm. (in press, 1991).
[17] T. Achibat, A. Boukenter, E. Duval, and B. Varrel (submitted).
[18] E. Duval, A. Boukenter, and B. Champagnon, Phys. Rev. Lett. **56**, 2052 (1986).
[19] W. W. Graessley and S. F. Edwards, Polymer **22**, 1329 (1981).
[20] T. A. Kavassalis and J. Noolandi, Macromolecules **22**, 2709 (1989).
[21] G. Lebourvellec, thesis, P.et M. Curie University, Paris, 1984.
[22] T. Achibat, A. Boukenter, and E. Duval (unpublished).
[23] D. G. H. Ballard, A. N. Burgess, J. M. Dekoninck, and E. A. Roberts, Polymer **28**, 3 (1987).
[24] A. J. Martin and W. Brenig, Phys. Status Solidi **64**, 163 (1974).
[25] A. Boukenter, B. Champagnon, E. Duval, J. Dumas, J. F. Quinson, and J. F. Serughetti, Phys. Rev. Lett. **57**, 2391 (1986).
[26] J. L. Rousset, A. Boukenter, B. Champagnon, J. Dumas, E. Duval, J. F. Quinson, and J. Serughetti, J. Phys. Condensed Matter **2**, 8445 (1990).
[27] A. B. Harris and A. Aharony, Europhys. Lett. **4**, 1355 (1987).
[28] M. G. Zemlyanov, V. K. Malinovsky, V. N. Novikov, P. P. Parshin, and A. P. Sokolov, JETP Lett. **51**, 314 (1990).
[29] A. Boukenter, E. Duval, and H. M. Rosenberg, J. Phys. C **21**, L541 (1988).

This article is copyrighted as indicated in the article. Reuse of AIP content is subject to the terms at: http://scitation.aip.org/termsconditions. Downloaded to IP: 137.189.170.231 On: Mon, 22 Dec 2014 19:13:10